Climate Change Impact On Flood Runoff Over Lake Baikal Catchment

Vadim Yurevich Grigorev (vadim308g@mail.ru)
Lomonosov Moscow State University https://orcid.org/0000-0001-8757-7344
Maxim A. Kharlamov
Lomonosov Moscow State University
Natalia K. Semenova
Lomonosov Moscow State University
Sergey R. Chalov
Lomonosov Moscow State University
Alexey A. Sazonov
Lomonosov Moscow State University

Research Article

Keywords: Baikal Lake catchment, flood flow, water balance, trend assessment

Posted Date: November 2nd, 2021

DOI: https://doi.org/10.21203/rs.3.rs-878531/v1

Abstract

Water level and distribution of dissolved and suspended matter of Lake Baikal are strongly affected by river inflow during rain-driven floods. This study analyses river flow changes at 44 streamflow gauges and related precipitation, evaporation, potential evaporation and soil moisture obtained from ERA5-Land dataset. Based on Sen-Slope trend estimator, Mann–Kendall non-parametric test, and using dominant analyses we estimated influence of meteorological parameters on river flow during 1979-2019. Using ridge-regression we found significant relationships between precipitation elasticity of river flow and catchments features. *Half* of the gauges in eastern part of Selenga river basin *showed* a significant decreasing trend of average and maximum river flow (up to -2.9%/year). No changes in central volume date of flood flow have been found. A reduction in rainfall amounts explains more than 60% of runoff decline. Decrease in evaporation is observed where precipitation decrease is 0.8%/y or more. Catchments where the precipitation *trends* are *not* as *substantial* are associated with increasing evaporation as a result of the increase of potential evaporation. Negative trends of precipitation are accompanied by negative trends of soil moisture. Finally, the study reveals sensitivity of the catchments with steep slopes in humid area to precipitation change.

Introduction

The impact of climate change on the hydrological regime of rivers is still a subject of active research in many part of the World (Ashmore and Church 2001; Mouri et al. 2013; Ehret et al. 2014), especially regarding extreme hydrological events such as floods or droughts (Renard et al. 2008). Long-term changes in water cycling in inland areas can considerably alter the hydrological and hydrogeochemical conditions of downstream lakes, wetlands and coastal waters. This is particularly important for the areas recently reported as the hot spots of ecosystem threats. One of them is the Lake Baikal area which contains 20% of the total amount of unfrozen freshwaters of the globe and thus representing unmatched source of freshwater in a drying world (Kasimov et al. 2019). River flow plays an important role for both economic activity and ecological condition of Baikal catchment (BC). Its magnitude, variability and timing reflect runoff-generation processes, including evapotranspiration, soil wetting-drying, permafrost freezing-thawing (Bring et al. 2015), erosion and weathering (Chalov et al. 2014), environmental functioning of streams (Goncharov et al. 2020) and wetlands (Thorslund et al. 2017). Direct monitoring these processes for large areas and long-term period is still hardly possible, particularly in developing countries like Russia and Mongolia (Karthe et al. 2014; Alekseevskii et al. 2015).

BC is the most economically developed part of Mongolia. Its area covers only 19% of the country's territory, whereas 75% (~ 2.5 million people) of total population and practically all industrial production is located here. Absence of the large impoundments within its basin supposes rather natural patterns of river flow (Chalov et al. 2014). Mining, industrial and agricultural activities within the Selenga drainage basin affect the flow generation processes which is additionally coveryd by overgrazing of pasture land, soil degradation and desertification (Onda et al. 2007; Garmaev et al. 2019). Russian part of BC is subjected to the crisis in the agricultural sector of the Russian economy in the end of 20th century and

associated abandonment of cultivated lands. Nevertheless, currently about 130 villages and towns (State report …, 2018) and 3000 km^2 of agricultural land under threat of flood (Kadetova and Radziminovich 2020). Currently, Lake Baikal is regulated as the part of the Irkutsk reservoir built in 1950–1959. Since 2001, level of Baikal is regulated not only by the Russian standard Regulations for the use of water resources of reservoirs, but also by a separate government decree limiting the permissible range of level fluctuations to 1 m, instead of 1.96 m laid down in the design (Abasov et al. 2017). Fulfillment of these requirements during low flow period of 1995–2017 led to economic damage, primarily due to a shortage of electricity generation at Angara river hydropower stations.

Long-term low flow period in BC is characterized by spring and summer flood flow reduction and average or above average minimum discharge (Frolova et al. 2017; Sinyukovich and Chernyshov 2019a). A comparison of the periods before and after 1975 in the Selenga basin showed overall trends of a decrease in the maximum (by 5–35%) and average annual runoff (up to 15%), with an increase in the minimum (by 30%), a decrease in the annual precipitation (by 12%) and evaporation despite an increase in potential evaporation (4%) (Frolova et al. 2017). Both a decrease in precipitation and permafrost thawing are considered as reasons for maximum runoff reduction (Törnqvist et al. 2014). Since 1971, a weak (~ 0.2% per year) tendency towards a decrease in the maximum runoff of rainfall floods is also characteristic of the Upper Angara and Barguzin rivers (Sinyukovich and Chernyshov 2017). Projections of the Selenga river flow change vary greatly and show both growth and decrease for different scenarios (Törnqvist et al. 2014; Pietroń et al. 2018).

The main driver of the observed hydrological changes in the regions probably is the increased frequency of anticyclogenesis (Antokhina et al. 2019). However, (Dorjsuren et al. 2018a) reported a slight increase in both summer and annual precipitation in the Mongolian part of the basin in 1979–2016, with a significant decrease in river runoff. Based on NCEP/NCAP reanalysis data (Sinyukovich and Chernyshov 2019b) reported that decrease of precipitation in 1971–2017 was insignificant, reaching 6 mm only in the southern part of the Selenga catchment area. Also, it was reported that the annual precipitation in the Mongolian part of the basin in 1996–2015 compared to 1978–1995 decreased from 300 mm to 272 mm, and the annual runoff decreased by 37%. A number of works mention the effect of evaporation on the annual runoff of the Selenga (Frolova et al. 2017; Sinyukovich and Chernyshov 2019a; Zorigt et al. 2019), without a detailed analysis of its impact.

These processes led to decreased sediment delivery to the Lake Baikal since the middle of the 1970s by 51% for the Selenga River and by 70% for the Upper Angara River and significant changes in sediment budget of the Selenga valley sink areas – downstream floodplains and delta (Chalov et al. 2018). Flooding of the wetland-dominated areas of the delta between the distributary channels occurs when Q > 3000 m^3/s (Aminjafari et al. 2020). Due to the decreased frequency of high discharge events (Q > 1350 m^3/s; Fig. 1), as well as the decreased magnitude of annual high flow events over the past two decades (Törnqvist et al. 2014), floodplain lakes could remain disconnected from the delta's main channels for longer time intervals, decreasing buffering functions of the delta (Chalov et al. 2017).

The recent estimates show that over 70% of suspended sediments are stored in the delta, including small particles that are important carriers of pollutants (Chalov et al. 2017; Pietroń et al. 2018; Roberts et al. 2020). Additionally, flood regime affects delta's macrophytes which capture from 3 up to 10%, heavy metals flow (Shinkareva et al. 2019). Finally, the impacts of the ambient conditions of riverine inflow to the Lake Baikal are linked to eutrophication of Lake Baikal waters which are in turn are related to 300% increase in chlorophyll concentration since 1979 and development of algae of the genus Spirogyra in the coastal zone (Kravtsova et al. 2014). The main factors determining the development of algae in Lake Baikal are the load of nitrogen and phosphorus (O'Donnell et al. 2017), while an increase in temperature, although it plays a positive role, does not have a significant effect. In turn, the phosphorus load by the Selenga River is regulated by the flood flow (Sorokovikova et al. 2018).Contribution of some particular drivers of river flow formation (topography, climate's aridity, features of the seasonal variation of precipitation and evaporation, type of vegetation cover) were never studied in the regional in sufficient quantitatively and sophisticated way (Merz et al. 2006; Guastini et al. 2019). At the same time it is supposed that their role can be important in average long-term runoff changes over BC region during 1950–2016 (Grigor'ev et al., 2020). Also, there is a lack of quantitative estimates of the particular climatic drivers impacts on abrupt changes in water delivery to Lake Baikal. Some studies showed importance of evaporation in flow decline (Sinyukovich and Chernyshov 2019b; Zorigt et al. 2019) but some stress the importance of precipitation (Frolova et al. 2017). Furthermore, it is remains unclear what cause evaporation change in BC on a basin scale (Minderlein and Menzel 2014).

This study aims to evaluate long-term flood flow change and related climate variables in the entire Lake Baikal catchment – both withing major and minor tributaries (in total 33 rivers) using more than 40 years of discharge observations and gridded climate data. In particular the study focuses on revealing trends in flood flow and associated climate variables; their relationships - quantifying the contribution of precipitation and evaporation to variability of floods and contribution of potential evaporation and soil moisture to evaporation; studying the connection between the geographical features of the catchments and the response of flood runoff to precipitation fluctuations.

Materials And Methods

Studied area

The climate of BC is continental, with dense snow cover during winter and warm and rainy summers. The average January temperature ranges from − 15°C to -25°C, while the average July temperature is around 14–18°C. At the same time, the average daily temperature can drop below − 40°C and rise above + 30°C. The mean precipitation in the Mongolian part of BC is about 300 mm, and in the Russian part it is more than 520 mm. In the river valleys of the Mongolian part of the basin, precipitation is less than 200 mm. In the mountains, the precipitation increases to 500 mm. In the Russian part of the basin, inequality is even greater – from less than 200 mm in river valleys and coastal areas of Lake Baikal to more than 1200 mm on the slopes of the Khamar Daban and Barguzinsky Ridges. The southern part of the BC is characterized by steppe vegetation, while the northern part is characterized by dense taiga. The main part of BC is

occupied by permafrost, mostly discontinuous and insular (The Ecological Atlas ..., 2015). In 1979–2016, the air temperature in the Mongolian and Russian parts of the BC increased by 1.8 °C and by 1 °C correspondingly. Analysis of transformation in the types of underlying surface for 2000–2010 revealed changes in the area of various types of underlying surface around 1000 km^2, i.e. about 0.2% of the BC area (Dorjsuren et al. 2018b).

We divided BC at 4 regions, according to their hydrographic features and available streamflow data (Fig. 2). The region I includes the upper reach of Selenga river basin above Naushki gauge near Mongolian-Russian border. The largest tributary of Selenga river in first area is Orkhon river, which occupies its eastern part. The lower part of the Selenga River basin is considered as region II. Within region II, the largest tributaries of the Selenga River are the Zheltura, Temnik (left-bank), Chikoy, Khilok, Uda (right-bank), splited by mountain ranges. To the North of the Temnik basin, catchments of small but water-bearing tributaries of the Baikal's South coast (region III) are located. To the North of the region II Turka, Barguzin and Upper Angara river basins are located (region IV).

Rain-dominated streamflows are most common for Selenga basin. Runoff formation within Mongolia is featured by the presence of altitudinal zoning, areas of runoff formation and disappearance. Runoff forms in the mountains, where it is facilitated by large slopes, low porosity and fracturing of rocks, and permafrost. The territory of the foothill plains is dominated by well permeable and not saturated alluvial and talus deposits. This leads to the absence of water inflow and water loss in the channel for infiltration (Garmaev et al. 2019).

Materials

44 stream gauges within BC from 1979 to 2019 were used in the present study. The daily discharges datasets from 1979 to 2007 were obtained from the Russian Federal Service for Hydrometeorology and Environmental Monitoring (Roshydromet) and are not publicly accessible. Data since 2008 are publicly available online from the Russian Federal Water Resources Agency.

Unfortunately, we were unable to obtain data on water discharge in Mongolia, what causes uneven distribution of gauges across the regions. Region II has 36 gauges available, whereas regions I, III, and IV have 1, 4, and 3 gauges respectively (Fig. 2). The gauges covered about 92% of BC area (excluding lake area) with median size of the considered watersheds is 3450 km^2. For seven gauges, there are gaps in the observations (primarily for 2002–2007). The share of missing values is 3.5% (Table 1).

Table 1
Gauges used in analysis and their characteristics

№	river	gauge	area, km2	missing years, %	Qmean	Qmax	CVD
1	Selenga	Naushki	282000	0	2.0	4.3	5-Aug
2	Selenga	Novoselenginsk	360000	0	3.5	6.4	5-Aug
3	Selenga	Mostovoy	440000	0	3.5	6.3	5-Aug
4	Selenga	Kabansk	445000	0	3.4	6.1	5-Aug
5	Chikoy	Chikoy	1340	2.5	20.6	98.1	30-Jul
6	Chikoy	Gremyachka	15600	0	12.7	40.5	3-Aug
7	Chikoy	Povorot	44700	2.5	10.6	23.6	5-Aug
8	Khilok	Mozgon	3240	0	2.4	9.7	1-Aug
9	Khilok	Khilok	15400	0	5.1	15.4	1-Aug
10	Khilok	Maleta	25700	0	4.7	11.7	1-Aug
11	Khilok	Malyy Kunaley	29600	0	4.9	13.8	1-Aug
12	Khilok	Khailastuy	38300	0	3.9	9.0	1-Aug
13	Djida	Khamney	8480	0	9.7	62.2	1-Aug
14	Djida	Djida	23300	0	8.6	34.2	7-Aug
15	Uda	Ust'-Egita	3900	2.5	2.7	16.1	31-Jul
16	Uda	Ulan-Ude	34700	0	2.9	7.8	30-Jul
17	Katantsa	Khilkotoy	2120	0	17.6	56.8	4-Aug

№	river	gauge	area, km2	missing years, %	Qmean	Qmax	CVD
18	Tsakirka	Sanaga	1030	0	16.0	129.6	1-Aug
19	Modonkul'	Zakamensk	138	0	13.9	188.3	5-Aug
20	Khamney	Khamneiskiy most	3600	0	11.7	79.0	2-Aug
21	Zheltura	Zheltura	5120	2.5	6.9	28.2	6-Aug
22	Temnik	Ulan-Udunga	4240	0	13.9	53.7	25-Jul
23	Kiran	Ust'-Kiran	1130	0	1.3	5.7	26-Jul
24	Ungo	Ust'-Ungo	2290	0	7.7	22.6	31-Jul
25	Balyaga	Petrovsk-Zabaykal'skiy	966	2.5	2.1	11.5	30-Jul
26	Bryanka	Zaigraevo	4190	10	1.5	3.1	28-Jul
27	Kuytunka	Tarbagatay	1060	0	0.7	3.6	1-Aug
28	Orongoy	Orongoiskiy most	1840	2.5	7.0	28.5	13-Jul
29	Kizhinga	Novokizhinginsk	820	7.5	2.3	9.1	2-Aug
30	Kudun	Mikhailovka	3300	0	3.9	10.6	2-Aug
31	Ona	Nizhnyaya Maila	2660	0	5.8	19.4	3-Aug
32	Malaya Kurba	Malaya Kurba	230	2.5	8.0	70.1	2-Aug
33	Kurba	Novaya Kurba	5500	2.5	7.0	19.3	25-Jul
34	Itantsa	Turuntuevo	2120	0	5.8	12.1	26-Jul
35	Atsa	Atsa	2010	2.5	15.8	51.5	1-Aug

№	river	gauge	area, km2	missing years, %	Qmean	Qmax	CVD
36	Bludnaya	Engorok	1300	0	8.8	45.0	1-Aug
37	Vilyuyka	Selenginsk	255	0	18.5	100.4	18-Jul
38	Bol'shaya Rechka	Posol'skaya	565	0	33.5	126.9	16-Jul
39	Snezhnaya	Vydrino	3000	22.5	31.3	123.2	27-Jul
40	Khara-Murin	Murino	1150	22.5	39.1	205.2	28-Jul
41	Utulik	Utulik	959	15	36.1	193.0	1-Aug
42	Verkhnyaya Angara	Verkhnyaya Zaimka	20600	0	27.6	61.3	12-Jul
43	Barguzin	Barguzin	19800	0	11.7	19.6	29-Jul
44	Turka	Sobolikha	5050	15	15.3	35.5	22-Jul

Discharge data on three gauges (№ 28, 29, and 32) are not available from 2016. Thus, in order to keep period of research uniform, we calculated missing values by linear regression with discharge on neighboring gauges. The average correlation coefficient between the datasets was 0.76.

The second dataset used in the analysis consists of climate variables – precipitation, evaporation, potential evaporation, and soil moisture in upper 28-cm layer. The dataset has been obtained from ERA5 Land (Muñoz-Sabater et al. 2021) for 1981–2019 and ERA-5 reanalysis for 1979–1980. ERA-5 is the fifth generation of the European Center for Medium-Range Weather Forecast (ECMWF) global weather reanalysis, using 4D variational assimilation in situ and remote sensing data (Hersbach et al. 2020). H-TESSEL (Tiled ECMWF Scheme for Surface Exchanges over Land) is the land surface model that is the basis of ERA-5 Land. A data from ERA5 in 1979–1980 for each grid cell was corrected by linear regression with ERA5-Land. The regression parameters were calculated for 1981–2019.

DEM MERIT Hydro dataset (Yamazaki et al. 2019), a digital elevation model, with removed critical errors for identifying watershed boundaries and flow direction, was selected to calculate catchments mean slopes and boundaries. The permafrost distribution was obtained from (Brown et al., 2002). The forest cover of the catchment was estimated using data from (Hansen and Song, 2018) based on satellite observations.

Methods

Data processing was carried out by free available soft: programming language Python and GIS QGIS.

We considered period from June to September as flood flow period. River flow was characterized by its volume (Q_{flood}) normalized by drainage area and expressed in liters per second from square kilometer, daily maximum discharge (Q_{max}), also expressed in liters per second from square kilometer, and flood period center-volume date (CVD, Julian date) for each year was calculated as the date when half of the total streamflow volume during the flood period passed by the gauge.

Precipitation (P) was characterized by its total amount and amount of heavy precipitation (P_{16} – above 16 mm/day) (Sato et al. 2007), and CVD. Evaporation (E), potential evaporation (PET), and soil moisture (W) data were averaged.

Also, for each region, for 1979–2019 average monthly terrestrial water storage change (TWSC) was calculated as (1)

$$\mathrm{TWSC} = \mathrm{P} - \mathrm{E} - \mathrm{Q} \, (1)$$

Sen's slope was used to determine the magnitude linear trends in hydrometeorological data. This slope is the median over all combinations of record pairs for the entire dataset (Helsel and Hirsch 2002). The statistical significance of the linear trends was assessed at α = 5%, 2%, and 1% level using the Mann–Kendall non-parametric test (Kendall 1975). The test doesn't assume probability distribution of the data that make him suitable for comparison highly distinguished watersheds.

Field significance was evaluated to assess if the Mann–Kendall test results in each of 4 regions were globally significant. For this we applied a modified Walker's test (Wilks 2016). The test evaluate if "global" null hypothesis that all individual "local" (gauges) null hypotheses are true. For each gauge within the area, the p-value of the local null hypotheses were calculated using the Mann–Kendall test. Further, p-values from N local hypothesis tests - p_i, were sorted in ascending order, so that $p_1 < p_2 \ldots < p_N$. Local null hypotheses were rejected if their respective p-values are no larger than a threshold level p_{FDR}

$$\mathrm{p_{FDR}} = \max \left[\mathrm{p_i} : \mathrm{p_i} \leq (\mathrm{i/N}) * \alpha_{\mathrm{FDR}} \right] (2)$$

If none of the sorted p-values satisfy the inequality in Eq. 2, then none of the respective null hypotheses can be rejected. Furthermore the size of that global hypothesis test (i.e., the probability of rejecting a global null hypothesis if it is true), is $\alpha_{global} = \alpha_{FDR}$. α was taken to be 5%

Dominance analysis approaches were applied to test the possible P and E impacts on Q_{flood} (Azen and Budescu 2003; Thomas and Famiglietti 2019), as well as W and PET influence on E. It was assumed that E does not cause a significant effect on P, the same as W is independent from PET. A number of studies show that for certain seasons and regions such a relationship exists, but it is usually weak, with Pearson's

correlation coefficients within 0.5 (Kislov et al. 2015; Duerinck et al. 2016; Zongxing et al. 2016). Based on this assumption, the effect of P on Q_{flood} is taken into account not only through the amount of available moisture, but also by reducing the PET on rainy days.

As part of the procedure for assessing the impact of P on Q_{flood} for each catchment, several multiple regression equations Q_{flood} (P, E) were compiled, where Q_{flood} was always taken for June-September, and P and E were taken with some delay (from 0 to 20 days), taking into account, that precipitation and evaporation from the catchment surface do not immediately affect the value of Q_{flood}. For further analyses, we used the most significant relationships based on coefficient of determination (R^2). For the same periods, which showed the highest R^2 value, linear trends P, P_{16}, E, PET, and W were calculated. The contribution of P to the variability of Q_{flood} was taken equals R^2 of the regression equation Q_{flood} (P). Similary, the contribution of E to the variability of Q_{flood} equals to the difference R^2 (Q_{flood} (P, E))–R^2 (Q_{flood} (P)).

The contribution of W and PET to the variability of E was calculated in a similar way. The contribution of W to the variability of E was counted as difference R^2(E (W, PET))–R^2(E (PET)), and the contribution from PET - as R^2(E (PET)).

Various catchments might pose a specific signals of climate changes to flood generation processes (Perdigão and Blöschl 2014). In particular, catchments may differ by the degree of Q_{flood} sensitivity to changes in P expressed through the ratio of the linear trend Q_{flood} (mm / year) to the linear trend P (mm / year) – ϵ_p. Due to the presence of errors in the P series, ϵ_p was calculated only for watersheds with the P trend, which is significant at the 5.6 % level. The percentage of area coveraged by permafrost of river basin, forests, non-forest vegetation, bare soil, the average slope of the catchment and the degree of climate humidity – the ratio of the average long-term value of P to E, were considered as the main climatic feature of river basins that affect ϵ_p (Table 2).

Table 2
Physical and geographical features of watersheds used in the study

Name	Variable	Dimension
PF	Permafrost	%
Fr	Forest	%
NFr	non-forest	%
BS	bare soil	%
S	mean slope	-
Hum	P/E	-

The influence of the features of river basins on the ϵ_p value was assessed using following statistical approach. Firstly, using the correlation matrix, we identified the parameters most closely related to ϵ_p, as well as the degree of dependence of these parameters on each other. Further, the graphs of the ϵ_p relationship from the selected characteristics were analyzed in order to find bouncing points associated with errors in the initial data or other factors not taken into account in the study. Next, a number of parameters have been transformed to linearize the relationship between them and ϵ_p. Finally, the correlation matrix was built again and the final selection of parameters for the model was carried out on its basis. Since changes in the features of catchments occur as a result of their coevolution, there is a correlation between them. Based on the ideas of cause-and-effect relationships in the formation of river runoff and landscapes, we chose the parameters that determine the value of ϵ_p.

To facilitate the search for the parameters of the regression dependence, all predictors were scaled. A significance of particular variables for explaining variability of ϵ_p was evaluated by F-test and t-test (Costa 2017) at 5% level.

Results

Water balance of the flood season. Despite the large spatial variation of amount precipitation during the flood period among 4 regions (from 310 mm in region I to 605 mm in region III), their seasonal distribution in BC is relatively similar. Maximal precipitation occurs in July – August and the minimal takes place in June or September. The September minimum are more pronounced for I and II regions. The maximum evaporation occurs earlier - in June – July with rapid decline in August – September (Fig. 3).

Maximum water discharge occurs after the maximum precipitation across region I and II, probable due to their vast area. Region III is characterized by a maximum water discharge in August, however, in contrast to the Selenga basin, water discharge in June and July practically does not differ from each other. Maximum of river discharge in region IV occurs in June further followed by decline during the entire season.

The TWS seasonality is different for each region. Our estimates predict minor growth of TWS in July – August and a slight decrease of TWS in June and September within region I. Such a small TWS variability compared to P and E is associated with vast closed-drainage area with a pronounced arid climate in BC, where large quantities of precipitated water are immediately lost by evaporation. Additionally, permafrost and steep slopes (Moreido and Kalugin 2017) hamper water storage capacity.

Region II is characterized by TWS reduction by about 20 mm in June and relative stability in the remaining months. Within region III TWS decrease in June reaches 50 mm, and for the entire flood period it is up 65 mm. The region IV is characterized by a decrease of TWS by 65 mm in June – July and an increase by 20 mm in August – September.

River flow change. Variability of river flow formation conditions in BC results in high spatial variability of flood discharges Q_{flood} – from 0.7 l/s*km^2 to 39.l/s*km^2 (Table 1) with coefficient of variation (the ratio of the standard deviation of the value to its mathematical expectation) from 0.25 to 1.2. Significant relationship with the Q_{flood} is observed (at the 0.1% significance level according to Mann-Kendall test).

Q_{max} consistently showed larger variability (from 3.2l/s*km^2 to 208 l/s*km^2) with coefficient of variation from 0.32 to 2.87 accordingly. Coefficient of variation of Q_{max} barely depends on catchments' area or Q_{max} mean value. The maximum values of the Q_{max} are observed in region III. The minimum values estimated here for the downstream of the Selenga and Uda rivers were close to maximum.

CVD of river flow varies from July 12 to August 6 (for 90% of the gauges from July 25), early for upper reaches of the basins and lately for lower ones. The exception is Upper Angara basin where the influence of melt runoff is significant (Sinyukovich and Chernyshov 2019b). Average standard deviation of CVD is about 12.5 days, up to 20 days in North-East part of region II and down to 9 days for gauges on Selenga river. Moreover, there is a significant relationship between coefficient of variation of Q_{flood} and coefficient of variation of the CVD (p-val = 0.12%).

Linear rates of change per year were determined by Sen slope estimate for Q_{flood}, Q_{max}, and CVD as well as their statistical significance by Mann-Kendall test. Q_{flood} showed the most consistent pattern of change with all study regions. 42 out of 44 gauges showed negative trend. The changes were significant at 5%, 2% and 1% level for 23, 14 и 11 gauges respectively. However, trends in regions III and IV were not field significant. The location of gauges with significant/insignificant trends and their magnitudes is depicted in Fig. 4.

All four gauges on Selenga river experienced downward trends, moreover, the rate of decrease is more pronounced at the downstream section and vary from − 1.08%/year at Naushki gauge near Mongolian-Russian border to -1.51% / year at Kabansk gauge. It can be seen that higher rates of Q_{flood} change at the lower reaches compared to the upper ones are also typical for the largest tributaries of the Selenga river in region II - the rivers Chikoy, Hilok and, to a lesser extent, Uda. These rivers as well as their tributaries and small rivers of North-East of region II showed maximum magnitude of Q_{flood} reduction. The trends in

Chikoy basin are around 0.7–1.4 %/year. Upper reaches of Hilok basin showed 1%/year Q_{flood} trend, whereas lower reaches are dominated by rate around 2%/year. The rate of Q_{flood} decrease for the northernmost tributaries of the Selenga river reaches 1.5–2.9% / year. Similarly, west part of region II is characterized mostly by Q_{flood} reduction, while none of the trends were significant. The rate of reduction is about 0.5%/year – up to 1%/year in upper reaches of the basins and at lower reaches is equals 0. Near the mouth of Djida river Q_{flood} trend reaches 0.4%/year (№ 14) – maximum value across all gauges. Region III had average Q_{flood} reduction rate around 0.6%/year with single gauge experienced statistically significant change (№ 38). Insignificant negative trends were found for the region IV, and the trend rate decreases from the South (around – 0.65%/year) to the North (-0.17%/year).

41 out of 44 gauges showed negative trend of Q_{max}, statistically significant at 5%, 2% and 1% level for 17, 9 and 6 gauges correspondingly. Overall, Q_{max} has similar to Q_{flood} rate of reduction and larger coefficient of variation. According to Mann-Kendall test, fewer gauges with significant Q_{max} trends compared to Q_{flood} were found. At the same time, unlike Q_{flood}, there is less pronounced change of Q_{max} trend downstream. Thus, the peaks of the maximum discharge have become more pronounced against the average flood peaks (Selenga, Uda, Hilok gauges). However, it is not the case for Chikoj and Turka rivers. Gauges with field significant changes of Q_{max} were determined only for region II. Nevertheless, there was the significant decreasing trend for Turka river in region IV.

Small number of gauges (2 out of 44) demonstrated significant CVD trend (not shown here). So, after the consideration of field significance herein, no significant trends were revealed for any region. 10 of 44 gauges had negative trend and located in North-East part of region II. Gauges with significant CVD trends (Itantsa and Bryanka rivers) also showed highest rate of Q_{flood} reduction (<-2.5%/год).

A negative relationship between Q_{flood} decline rate and average elevation of catchment was revealed (p-val < 5%). The connection is probably associated with an increase of average Q_{flood} value with an increase in the average catchment height.

Precipitation and evaporation influence on river flow variation. A strong connection between P and E with Q_{flood} revealed R^2(P, E) median equals 0.66 (Fig. 5). Precipitation is a most important factor influencing Q_{flood} in BC. A median R^2(P) value is 0.63, while minimum 0.34 and maximum 0.79.

The contribution of evaporation is by order of magnitude less important: the median R^2(E) estimated here is 0.022, with a minimum close to 0 and a maximum of 0.12. Furthermore, the median value of the E / P ratio is 0.9. E and P average values are similar. Low values of R^2 (E) can be due to many different reasons (E may be more changeable where river flow is close to zero; moisture loss from upper soil level may does not affect much river flow formation in June–September; errors in initial E data etc.). We considered two of them:

1) E value during flood season is almost completely determined by the value of P, and

2) the variability of E is much less than the variability of P.

In general, for the BC, there is a weak positive relationship between P and E - the median value of the Pearson correlation coefficient (r) is 0.34. Moreover, more than half of the gauges (25 out of 44) had positive r value. Probably, the sign of r is determined by the main limiting factor of evaporation in the basin - the available moisture (in this case, $r > 0$) or potential evaporation ($r < 0$) (Jung et al. 2010). It seems like the small value of R^2 (E) is explained mostly by the low variability of E – the median ratio standard deviation of E to standard deviation of P is 0.28. Thus, E control amount of available for runoff formation water at much less extent that P.

The three lower gauges on the Selenga river have R^2(P) value around 0.71–0.76. The upper gauge (Naushki) has R^2(P) value 0.59. This is consistent with vast closed drainage regions in region I, precipitation of that have been taken into account for region I precipitation amount. Overall, the minimum values of R^2(P) in the region II were observed in the western part of the area, where they are 0.4–0.5. Hilok, Uda and Chikoy rivers have R^2(P) values around 0.7–0.75.

Gauges of region III have R^2(P) values close to those of western part of II area (0.53–0.58), with the exception of the Utulik river, where R^2(P) is 0.34. In the region IV the Turka river showed R^2(P) value typical for the eastern part of II area (0.69), while the Barguzin and Upper Angara rivers showed almost identical results – 0.50 and 0.52.

It can be seen that most of the gauges have R^2(E) values less than 0.06. Some exceptions here are two rivers of region III - Khara-Murin amd Snezhnaya with R^2(E) equal to 0.11 and 0.12 accordingly.

Precipitation change. All catchments showed decreasing trends in P with spatial distribution of linear trend rate similar to Q_{flood}. The rate of P decline in region I was 0.65% / year (p-val = 0.1%). Western part of region II showed rate of P decline ranging between − 0.25%/year to -0.45%/year. Though, the trend was significant only for one watershed at p-val < 5%. The upper reaches of the Chikoy river are characterized by a linear trend of -0.55 – -0.65% / year. The downstream gauges over there have P decline rate up to -0.8–0.9%/year. Hilok basin is characterized P trend rate around − 0.7 – -1% / year, with large trend rate located in downstream. The highest rates of P decrease have been shown in the Uda basin – -1 – -1.5% / year, regardless of the position within the catchment, except for the upper gauge where P rate is -0.7%/year. Three of four catchments of region III have P decline rate about − 0.45% / year. However, a catchment located near Selenga delta (Table 1, №38) showed decline rate around − 1.1% / year. The region IV is characterized by a decrease in the linear trend of P magnitude from south to north - from − 1% / year in the Turka catchment and up to -0.1% in the Upper Angara catchment (Table 3). Overall, the decrease in the precipitation amount is statistically significant for I and II regions, with the median p-val across all 44 catchments being 0.03%. Like for Q_{flood}, significant changes of P CVD for 1979–2019 was not identified - the median value of p-val of the CVD P linear trend was 66.4%, with a minimum of 9%.

Linear trends of P_{16} for 40 river basins were negative (Table 3), however, due to the greater variability of P_{16} compared to P, they were statistically significant only for the regions of the Turka and Kurba rivers (border of regions II and III). Generally, the rate of P_{16} decline is less than that for P. The ratio of the median of the P_{16} trend to the median of the P trend is 0.92. This could be the reason why the negative trend of Q_{max} is slightly less than for Q_{flood}.

Table 3
Linear rates of changes P, P16, E, PET and W for BC river basins, %/year. *Italic* – significant at 5%, **bold** – at 1%.

№	P	E	PET	P_{16}	W
1	**-0.65**	**-0.18**	**0.43**	-0.46	**-0.55**
2	**-0.69**	*-0.15*	**0.46**	-0.40	**-0.51**
3	**-0.71**	**-0.21**	**0.48**	-0.57	**-0.54**
4	**-0.71**	**-0.21**	**0.49**	-0.57	**-0.54**
5	*-0.55*	**0.27**	**0.44**	-0.16	**-0.20**
6	*-0.61*	*0.12*	**0.58**	-0.30	**-0.37**
7	**-0.72**	0.03	**0.64**	-0.54	**-0.42**
8	*-0.78*	-0.11	**0.51**	-0.48	**-0.61**
9	*-0.64*	-0.12	**0.56**	-0.31	**-0.53**
10	**-0.78**	*-0.17*	**0.58**	-0.88	**-0.53**
11	**-0.80**	*-0.19*	**0.60**	-0.90	**-0.53**
12	**-0.94**	**-0.30**	**0.60**	-0.82	**-0.55**
13	-0.29	**0.21**	**0.37**	-0.16	**-0.20**
14	-0.33	-0.02	**0.41**	0.00	**-0.29**
15	*-0.70*	-0.32	**0.60**	0.32	**-0.62**
16	-1.16	**-0.44**	**0.60**	-1.36	**-0.75**
17	-0.86	*0.14*	**0.67**	-0.82	**-0.26**
18	*-0.46*	**0.23**	**0.31**	-0.26	**-0.17**
19	-0.27	*0.13*	**0.30**	0.34	*-0.25*
20	-0.35	**0.21**	**0.37**	-0.15	**-0.22**
21	-0.22	0.05	**0.35**	0.71	*-0.26*
22	-0.51	*0.14*	**0.52**	-0.36	**-0.28**
23	*-0.83*	**-0.83**	**0.55**	-1.31	**-0.71**
24	**-0.86**	-0.05	**0.61**	-0.99	**-0.42**
25	**-1.21**	**-0.82**	**0.60**	-0.75	**-0.84**
26	**-1.34**	**-0.68**	**0.64**	-1.43	**-0.81**

№	P	E	PET	P_{16}	W
27	**-1.46**	**-1.03**	**0.75**	-1.52	**-0.75**
28	**-1.22**	*-0.33*	**0.69**	-1.25	**-0.60**
29	**-1.10**	**-0.53**	**0.59**	-1.51	**-0.75**
30	**-0.98**	*-0.33*	**0.55**	-0.64	**-0.70**
31	**-1.32**	-0.14	**0.64**	*-1.87*	**-0.71**
32	**-1.16**	-0.07	**0.69**	**-2.10**	**-0.63**
33	**-1.14**	-0.05	**0.57**	*-2.02*	**-0.55**
34	**-1.24**	-0.06	**0.70**	*-2.01*	**-0.49**
35	*-0.64*	*0.17*	**0.62**	-0.54	**-0.31**
36	**-0.79**	0.07	**0.48**	-1.22	**-0.37**
37	**-1.27**	0.00	**0.73**	-1.54	**-0.51**
38	**-1.09**	0.14	**0.68**	-1.43	**-0.32**
39	*-0.42*	**0.34**	**0.48**	-0.26	**-0.11**
40	**-0.45**	**0.35**	**0.48**	-0.61	**-0.06**
41	*-0.41*	**0.30**	**0.46**	-0.55	**-0.06**
42	-0.09	**0.33**	**0.43**	-0.14	-0.01
43	*-0.66*	**0.22**	**0.52**	-0.94	**-0.18**
44	**-0.99**	**0.30**	**0.66**	**-2.17**	**-0.23**

Evaporation change. The spatial pattern of E trend is much more unequal compared to P or Q_{flood}. E change rates vary from − 1.03%/year to 0.35%/year. In general, the catchment with negative P trends less than 0.8%/year indicate positive E trend. These examples include West part of region II, the upper reaches of the Hilok and Chikoy rivers, region III and northern part of region IV. A decrease in E is typical for catchments where more than 0.8%/year P decrease was observed. Overall, regions I and II showed the rate of E decrease about 0.2–0.3%/year, III region showed growth around 0.4%/year and in IV region E trend around − 0.25–0.4%/year is observed. In humid catchments, against the background of a decrease in precipitation, an increase in the amount of evaporation occurred. Within the region III, the value of E increased, even for the catchment area where the decrease in P reached 1.1% / year

Due to the small value of the E variability, even relatively small values of the E rate change (around 0.2% per year) are statistically significant. As a result, the changes in E are statistically significant for all 4

regions, however, if in the regions III and IV (increase in E) and in the I area (decrease in E) they are unidirectional, then for the II area they are multidirectional (Table 3).

It is likely that an increase in E in some catchments despite a decrease in P is associated with an increase in PET. Spatial distribution of PET trend is similar to the P, but with opposite sign. That is probably due to small PET value on days with precipitation. Region I showed the growth rate of PET at 0.43% / year. The minimum values of the PET trend across study region took place in the Jida river basin where they are equal to 0.3–0.4% / year. However, further North, in the Temnik river basin and in the south of the III region, they are 0.5% / year. The trend values are already 0.5–0.7% / year in the east part of the II area and the north of the III region. In region IV, the trend decreases from 0.66%/year in the south to 0.43%/year in the north.

On the other hand, decrease of W led to decline in evaporation moisture availability. The only catchment where decrease of W was unsignificant was the Upper Angara catchment. Other catchments showed W trend significant at 5% level. There are many more catchments that exhibit a trend than would be expected to occur by chance. Due to the low variability of W, the median value of the W trend is only 0.5%/year. The lowest rate of decrease of W was detected in Southern part of region III (0.05–0.1%), and the maximum in the Uda basin (0.6–0.8% per year). Overall, the features of the spatial pattern of the W change are similar to the change of Q_{flood} and P.

E is closely related to PET and W in most catchments. The median value of R^2(PET, W) was 0.56, with the contribution of PET being equal to 0.36. The minimum values of R^2(PET, W) were obtained from Chikoy river (R^2(PET, W) = 0.15). The maximum values of R^2(PET, W) (0.81–0.91), as well as R^2 (PET) (0.79–0.88), were obtained from catchments with the highest precipitation amount (Upper Angara, South of the region III).

Connection between precipitation elasticity of river flow and watersheds features. The number of catchment evaluated for connection between precipitation elasticity of river flow (ϵ_p) and catchments features (32) was less than that used in P and Q_{flood} determination because of the fact that some catchments demonstrated statistically insignificant P change rate (below 5.6%), either were too vast, so value averaged over entire basin is not representative (Selenga river's gauges).

The two catchments located in the Northwest of the Baikal basin (Khara-Murin and Snezhnaya) have ϵ_p close to 1–0.95 and 0.8 accordingly. Due to the small size of these basins (up to 3000 km^2), this may be because of initial data uncertainties. However, since these catchments related to the humid climates (P/PET ratio is from 1.23 to 2.08) and continuous permafrost region, ϵ_p around 1 is physically possible. In particular, the amount of precipitation of humid areas is less connected with the amount of evaporation - r between P and E for these three catchments varies from 0.07 to 0.14. Also precipitation, not only themselves form river flow, but also contribute to the melting of permafrost, which leads to an increase in moisture available for the formation of river flow.

The median value of ϵ_p was 0.29, with a minimum of 0.03. Such a relatively low sensitivity of Q_{flood} to P, while PET is increasing that should enhance Q_{flood} decline due to P decline, can be explained by relatively arid climate of the considered are with median Hum equal to 1.07. So, a more definite analysis requires consideration of the water balance of the catchments in other seasons.

The correlation matrix of untransformed features of catchments and ϵ_p is given in Fig. 6.

For further study, we elaborated specific indices for the catchment parameters demonstrating a monotonic relationship with ϵ_p, aiming to reach linear functions with ϵ_p. In particular, the BS was transformed

$$\mathrm{Fr}' = \frac{\sqrt{\mathrm{Fr} - 20}}{10}$$

and S

$$\mathrm{S}' = \frac{1}{10}\mathrm{S}^2 + \frac{1}{10}\mathrm{S}.$$

After linearization features S' and BS' the correlation rate band etween them and ϵ_p will be equal 0.44 and 0.82 respectively. Hence, there is strong positive correlation between ϵ_p and the following features: S', Hum, PF, BS, and Fr'. These four variables had R^2 around 0.67, 0.52, 0.21, 0.19 and 0.19 accordingly. After evaluation the significance of the variables by F-test and t-tset, the following features were taken for the model: S' and BS.

The following model was obtained:

$$\epsilon_p \mathrm{predicted} = 0.229 + 0.0057 \bullet \mathrm{S}' - 0.0348 \bullet \mathrm{BS} \; (3)$$

explaining about 74% of the ϵ_p variability (Fig. 7).

Discussion

Our results significantly extend the previous finding related to climate change impact on hydrological system in the regional Baikal catchment. They suggest significant spatial heterogeneity of hydroclimatic development in the region.

June and July in regions II, III, and IV are characterized by highest in a season precipitation but decreasing of TWS. Mostly arid conditions and low snow cover, the main considered driver of these changes might be the melting of seasonally frozen ground (Sazonova et al. 2004; Biskaborn et al. 2019). Towards the middle of summer, the lower portion of the permafrost is still not subjected to melting. Further replacement of the underground ice by rainwaters is observed. However, this conclusion is based

on assumption of unbiased estimate of difference between P and E in ERA5-Land, that may not be a case. ERA5 (and ERA5-Land accordingly) has tendency to overestimate P (Nogueira 2020) and ERA5-Land has tendency to overestimate E (Muñoz-Sabater et al. 2021). A calculated river discharge of Selenga river based on ERA5-Land (Harrigan et al. 2020) has bias around 20%, thus ERA5-Land has rather positive bias of P–E. So it is likely that our estimate of TWS decline during June–August in the regions is underestimated.

The decrease of P, Q_{flood} and Q_{max} is most pronounced over region I, eastern part of the region II, northern part of region III and southern part of the region IV. This pattern is consistent with the early findings (Antokhina et al. 2019), wherein runoff decrease in the Selenga basin was associated with middle summer precipitation decrease, which is impacted by weakening of the East Asian summer monsoon. However, we found no evidence of altering temporal pattern of precipitation and river flow during June–September. Also it can be seen that P obtained in this study from ERA5 showed much more rapid P decline then the one obtained from precipitation gauges (Dorjsuren et al. 2018b, a; Zorigt et al. 2019).

We did not have data on daily river discharges within the Mongolian part of the basin (practically the region I) and we do not know any publications containing their analysis, however, indirectly, a decrease in the flood runoff in the Mongolian part of the basin is indicated by a decrease in the annual runoff for 1979–2016 [Dorjsuren et al., 2018 b] and 1978–2015. [Zorigt et al., 2019], the most significant for the South part of the region.

Our results reflect strong connection between Q_{flood} and P in Baikal basin. Despite some recent changes in air temperature (Törnqvist et al. 2014), land cover (Dorjsuren et al. 2018b) and water demand (Garmaev et al. 2019) precipitation variation still explains up to 80% of Q_{flood} variation. However, correctness of the conclusion depends on accuracy of long-term precipitation change in ERA5. Some other works, based on NCEP/NCAP reanalysis (Sinyukovich and Chernyshov 2019b) or meteostations' observations (Zorigt et al. 2019) emphasized increase of evaporation and potential evaporation as key factors of river flow decline. The assessment of accuracy of ERA5 P linear trend (Sun et al. 2020) showed minor (about 1 mm/year) bias for northeastern part of China, that is near BC.

In general, for the BC, there is a weak positive relationship between P and E - the median value of the Pearson correlation coefficient (r) is 0.34. Moreover, more than half of the gauges (25 out of 44) had positive r value. Probably, the sign of r is determined by the main limiting factor of evaporation in the basin - the available soil moisture (in this case, $r > 0$) or potential evaporation ($r < 0$) (Jung et al. 2010). So, It seems like the small value of R2 (E) is explained mostly by the low variability of E – the median ratio standard deviation of E to standard deviation of P is 0.28.

The rate of precipitation's change is spatially inhomogeneous and can vary by a factor of two or more for catchments located at a distance of 150–250 km from each other (Table 3, Fig. 1). The obtained trends and their statistical significance are indicators of current changes of flow formation, but cannot be used to predict its changes in the future. Despite the general downward trend of Q_{flood} in the Baikal basin over

the past decades, the Q_{flood} was higher or close to the norm for some current years (2012, 2013, 2018, 2019). Also, according to preliminary data, the river flow was higher or close to the norm in 2020–2021.

Slightly less intense of P_{16} decrease compare annual P values explains increase in temporal inequality of P distribution in Baikal basin. This is in line with global trends explained by climate change impacts (Pendergrass and Knutti 2018). The alter of precipitation distribution partly explains Q_{flood} and Q_{max} decrease at similar rate.

Heterogeneous patterns of E change (Table 3) are most probably associated with, decline of W, and growth of PET values. The increase of PET in Baikal basin can be associated not only with global trends - an increase in direct solar radiation, as a result of a «global brightening» (He et al. 2018), and an increase of vapor pressure deficit, as a result of growing air temperature (Algarra et al. 2020), but also with a decrease in the number of days with precipitation. Statistical analysis showed that PET plays the main role in the variability of E (about 36%), and the role of W is secondary (about 19%). However, it is important to note that PET, like W, show significant trends, and it is impossible to separate their influence solely by statistical methods.

Multiple linear regression showed that the large ϵ_p values are features of whose catchments that are distinguished by a large slopes and small bare soil area (Fig. 7). Catchments characterized by these features usually have runoff coefficient more than the other ones. Also it can be seen that at the basin scale topography is more important than climate for particular response of flood flow to climate change. These outcome is close to the conclusions from an earlier research examining hydrological drought variation (Van Loon and Laaha 2015). Since ϵ_p depends mostly on terrain features we can assume that relationship between Q and P will keep being linear in changing climate and altering land use.

Our results suggest that precipitation variability remains main factor of rain-driven floods variability in BC, despite both the rise in air temperature and solar radiation (He et al. 2018; Dorjsuren et al. 2018b). Precipitation regulates both Q and E not only by amount of available water but also by PET rate. So, median correlation coefficient between P and PET among 44 river basins is < − 0.8. The result is similar to what was obtained on a global scale (Jung et al. 2010) where W was considered as main factor of E change. The conclusion also suggests that accuracy of P in climate projections is the key factor for assessment of future water resources in BC.

Conclusion

The nonstationarity of the flood flow in the Baikal basin, as well as the peculiarities of the catchments' response to climatic changes, depending on their characteristics, should be taken into account when planning economic activities in this region. In particular, this is crucially important due to future possible hydropower projects development and Lake Baikal water level regulation.

1. The flood runoff over Baikal catchment is one of the most important environmental drivers effecting pristine ecosystem of the largest freshwater reservoir of the World. From 1979 to 2018, the Q_{flood} and Q_{max} showed decreasing trend under the influence of a precipitation decreasing. The most substantial changes were revealed in the northeastern part of the Selenga basin with the rates up to 1.5–2%/year. There was no clear signal of altering river flow timing during June–September with slight domination of upward CVD river flow trends. The decrease of precipitation affected the entire catchment area of Lake Baikal. A P_{16} (P> 16 mm / day) did not decrease as much (by 8% less) than the total precipitation, i.e. their distribution became more uneven. A statistically significant negative trend of evaporation was revealed for 15 catchments (up to -1.03%/y), and a positive one for another 15 (up to 0.35%/y). Statistically most significant changes occurred with soil moisture and potential evaporation. A significant decline of W was revealed for 43 from 44 river basins with exception of Upper Angara basin. An increase of PET has place over entire BC with p-val<1%.
2. Q_{flood} showed a close relationship to P – the median value of the coefficient of determination was 0.63. The impact of E variation on Q_{flood} variation was rather neglectable. Due to the comprehensive impact of the increasing potential evaporation and decreasing soil moisture, the amount of evaporation has changed over the studied period. A decrease in evaporation is typical for catchments that have experienced a decrease in P by more than 0.8% per year and where the amount of available moisture can limit the evaporation.
3. Statistical analysis revealed that Q_{flood} of watersheds with large steep slopes and small bare soil area are most sensitive to alter of P. Since depends mostly on terrain features, first of all on slope, we can assume that relationship between Q and P will keep being linear in changing climate and altering land use.

Declarations

Funding The study was supported by Russian Fund for Basic research projects 18-05-80094. Additionally, the research was performed according to the Development program of the Interdisciplinary Scientific and Educational School of M.V. Lomonosov Moscow State University (Future Planet and Global Environmental Change)

Conflicts of interest Not applicable

Availability of data and material All datasets except river discharge using or analyzed in this study are publicly available. River discharge data are available from the corresponding author on reasonable request.

Code availability Not applicable

Ethics approval Not applicable

Consent to participate Not applicable

Consent for publication Not applicable

References

1. Abasov NV, Bolgov MV, Nikitin VM, Osipchuk EN (2017) Level regime regulation in Lake Baikal. Water Resour 2017 443 44:537–546. https://doi.org/10.1134/S0097807817030022
2. Alekseevskii NI, Zavadskii AS, Krivushin MV, Chalov SR (2015) Hydrological monitoring at international rivers and basins. Water Resour 42:747–757. https://doi.org/10.1134/S0097807815060020
3. Algarra I, Nieto R, Ramos AM et al (2020) Significant increase of global anomalous moisture uptake feeding landfalling Atmospheric Rivers. Nat Commun 2020 111 11:1–7. https://doi.org/10.1038/s41467-020-18876-w
4. Aminjafari S, Brown I, Chalov S et al (2020) Temporal and Spatial Changes of Water Occurrence in the Selenga River Delta. https://doi.org/10.1002/ESSOAR.10504519.1
5. Antokhina OY, Latysheva IV, Mordvinov VI (2019) A cases study of mongolian cyclogenesis during the July 2018 blocking events. Geogr Environ Sustain 12:. https://doi.org/10.24057/2071-9388-2019-14
6. Ashmore P, Church M (2001) The impact of climate change on rivers and river processes in Canada. Bull Geol Surv Canada. https://doi.org/10.1126/science.1189930
7. Azen R, Budescu DV (2003) The Dominance Analysis Approach for Comparing Predictors in Multiple Regression. Psychol Methods 8:129–148. https://doi.org/10.1037/1082-989X.8.2.129
8. Biskaborn BK, Smith SL, Noetzli J et al (2019) Permafrost is warming at a global scale. Nat Commun 2019 101 10:1–11. https://doi.org/10.1038/s41467-018-08240-4
9. Bring A, Asokan SM, Jaramillo F et al (2015) Implications of freshwater flux data from the CMIP5 multimodel output across a set of Northern Hemisphere drainage basins. Earth's Futur 3:206–217. https://doi.org/10.1002/2014EF000296
10. Brown J, Ferrians O, Heginbottom JA, Melnikov E (2002) Circum-Arctic Map of Permafrost and Ground-Ice Conditions, Version 2. Boulder, Colorado USA. NSIDC: National Snow and Ice Data Center. doi: https://doi.org/10.7265/skbg-kf16. [05.05.2019]
11. Chalov S, Thorslund J, Kasimov N et al (2017) The Selenga River delta: a geochemical barrier protecting Lake Baikal waters. Reg Environ Chang 17:2039–2053. https://doi.org/10.1007/s10113-016-0996-1
12. Chalov SR, Jarsjö J, Kasimov NS et al (2014) Spatio-temporal variation of sediment transport in the Selenga River Basin, Mongolia and Russia. Environ Earth Sci 73:. https://doi.org/10.1007/s12665-014-3106-z
13. Chalov SR, Millionshchikova TD, Moreido VM (2018) Multi-Model Approach to Quantify Future Sediment and Pollutant Loads and Ecosystem Change in Selenga River System. Water Resour 45:22–34. https://doi.org/10.1134/S0097807818060210

14. Dorjsuren B, Yan D, Wang H et al (2018a) Observed trends of climate and river discharge in Mongolia's Selenga sub-basin of the Lake Baikal basins. Water 10:1436. https://doi.org/10.3390/w10101436
15. Dorjsuren B, Yan D, Wang H et al (2018b) Observed trends of climate and land cover changes in Lake Baikal basin. Environ Earth Sci 77:725. https://doi.org/10.1007/s12665-018-7812-9
16. Duerinck HM, van der Ent RJ, van de Giesen NC et al (2016) Observed soil moisture-precipitation feedback in Illinois: A systematic analysis over different scales. J Hydrometeorol 17:1645–1660. https://doi.org/10.1175/JHM-D-15-0032.1
17. Ehret U, Gupta HV, Sivapalan M et al (2014) Advancing catchment hydrology to deal with predictions under change. Hydrol Earth Syst Sci 18:649–671. https://doi.org/10.5194/hess-18-649-2014
18. Frolova NL, Belyakova PA, Grigoriev VY et al (2017) Runoff fluctuations in the Selenga River Basin. Reg Environ Chang 17:1965–1976. https://doi.org/10.1007/s10113-017-1199-0
19. Garmaev EZ, Bolgov MV, Ayurzhanaev AA, Tsydypov BZ (2019) Water Resources in Mongolia and Their Current State. Russ Meteorol Hydrol 44:659–666. https://doi.org/10.3103/S1068373919100030
20. Goncharov AV, Baturina NS, Maryinsky VV et al (2020) Ecological assessment of the Selenga River basin, the main tributary of Lake Baikal, using aquatic macroinvertebrate communities as bioindicators. J Great Lakes Res 46:53–61. https://doi.org/10.1016/j.jglr.2019.11.005
21. Grigor'ev VYu, Millionshchikova TD, Sazonov AA, Chalov SR (2020) Impact of changes in the main climatic parameters on river runoff in the Baikal Lake basin during the second half of the 20th and the early 21st century. Vestnik Moskovskogo universiteta. Seriya 5, Geografiya (5):3–11. (In Russ.)
22. Guastini E, Zuecco G, Errico A et al (2019) How does streamflow response vary with spatial scale? Analysis of controls in three nested Alpine catchments. J Hydrol 570:705–718. https://doi.org/10.1016/j.jhydrol.2019.01.022
23. Hansen M, Song X: Vegetation Continuous Fields (VCF) Yearly Global 0.05 Deg, Data set, https://doi.org/10.5067/MEaSUREs/VCF/VCF5KYR.001, 2018
24. Harrigan S, Zsoter E, Alfieri L et al (2020) GloFAS-ERA5 operational global river discharge reanalysis 1979-present. Earth Syst Sci Data 12:2043–2060. https://doi.org/10.5194/ESSD-12-2043-2020
25. He Y, Wang K, Zhou C, Wild M (2018) A Revisit of Global Dimming and Brightening Based on the Sunshine Duration. Geophys Res Lett 45:4281–4289. https://doi.org/10.1029/2018GL077424
26. Helsel DR, Hirsch RM (2002) Statistical methods in water resources
27. Hersbach H, Bell B, Berrisford P et al (2020) The ERA5 global reanalysis. Q J R Meteorol Soc 146:1999–2049. https://doi.org/10.1002/qj.3803
28. Jung M, Reichstein M, Ciais P et al (2010) Recent decline in the global land evapotranspiration trend due to limited moisture supply. Nat 2010 4677318 467:951–954. https://doi.org/10.1038/nature09396

29. Kadetova AV, Radziminovich YB (2020) Historical floods within the Selenga river basin: chronology and extreme events. Nat Hazards 2020 1031 103:579–598. https://doi.org/10.1007/S11069-020-04001-Z
30. Karthe D, Chalov S, Borchardt D (2014) Water resources and their management in central Asia in the early twenty first century: status, challenges and future prospects. Environ Earth Sci 73:487–499. https://doi.org/10.1007/s12665-014-3789-1
31. Kasimov N, Kosheleva N, Lychagin M et al (2019) Environmental Atlas Selenga-Baikal. Faculty of Geography, Lomonosov Moscow State University, Moscow
32. Kendall M (1975) Rank correlation measures. Charles Griffin, London
33. Kislov AV, Varentsov MI, Tarasova LL (2015) Role of spring soil moisture in the formation of large-scale droughts in the East European Plain in 2002 and 2010. Izv - Atmos Ocean Phys 51:405–411. https://doi.org/10.1134/S0001433815020061
34. Kravtsova LS, Izhboldina LA, Khanaev IV et al (2014) Nearshore benthic blooms of filamentous green algae in Lake Baikal. J Great Lakes Res 40:441–448. https://doi.org/10.1016/j.jglr.2014.02.019
35. Merz R, Blöschl G, Parajka J (2006) Spatio-temporal variability of event runoff coefficients. J Hydrol 331:591–604. https://doi.org/10.1016/j.jhydrol.2006.06.008
36. Minderlein S, Menzel L (2014) Evapotranspiration and energy balance dynamics of a semi-arid mountainous steppe and shrubland site in Northern Mongolia. Environ Earth Sci 2014 732 73:593–609. https://doi.org/10.1007/S12665-014-3335-1
37. Moreido VM, Kalugin AS (2017) Assessing possible changes in Selenga R. water regime in the XXI century based on a runoff formation model. Water Resour 44:390–398. https://doi.org/10.1134/S0097807817030149
38. Mouri G, Minoshima D, Golosov V et al (2013) Probability assessment of flood and sediment disasters in Japan using the total runoff-integrating pathways model. Int J Disaster Risk Reduct 3:31–43. https://doi.org/10.1016/j.ijdrr.2012.11.003
39. Muñoz-Sabater J, Dutra E, Agustí-Panareda A et al (2021) ERA5-Land: A state-of-the-art global reanalysis dataset for land applications. Earth Syst Sci Data Discuss 1–50. https://doi.org/10.5194/ESSD-2021-82
40. Nogueira M (2020) Inter-comparison of ERA-5, ERA-interim and GPCP rainfall over the last 40 years: Process-based analysis of systematic and random differences. J Hydrol 583:124632. https://doi.org/10.1016/j.jhydrol.2020.124632
41. O'Donnell DR, Wilburn P, Silow EA et al (2017) Nitrogen and phosphorus colimitation of phytoplankton in Lake Baikal: Insights from a spatial survey and nutrient enrichment experiments. Limnol Oceanogr 62:1383–1392. https://doi.org/10.1002/lno.10505
42. Onda Y, Kato H, Tanaka Y et al (2007) Analysis of runoff generation and soil erosion processes by using environmental radionuclides in semiarid areas of Mongolia. J Hydrol 333:124–132. https://doi.org/10.1016/j.jhydrol.2006.07.030

43. Pendergrass AG, Knutti R (2018) The Uneven Nature of Daily Precipitation and Its Change. Geophys Res Lett 45:11,980 – 11,988. https://doi.org/10.1029/2018GL080298
44. Perdigão RAP, Blöschl G (2014) Spatiotemporal flood sensitivity to annual precipitation: Evidence for landscape-climate coevolution. Water Resour Res 50:5492–5509. https://doi.org/10.1002/2014WR015365
45. Pietroń J, Nittrouer JA, Chalov SR et al (2018) Sedimentation patterns in the Selenga River delta under changing hydroclimatic conditions. Hydrol Process 32:278–292. https://doi.org/10.1002/hyp.11414
46. Plyusnin VM (ed) (2015) The Ecological Atlas of the Baikal Basin. V.B. Sochava Institute of Geography, Irkutsk, Russia
47. Renard B, Lang M, Bois P et al (2008) Regional methods for trend detection: Assessing field significance and regional consistency. Water Resour Res 44:. https://doi.org/10.1029/2007WR006268
48. Roberts S, Adams JK, Mackay AW et al (2020) Mercury loading within the Selenga River basin and Lake Baikal, Siberia. Environ Pollut 259:113814. https://doi.org/10.1016/j.envpol.2019.113814
49. Sato T, Kimura F, Kitoh A (2007) Projection of global warming onto regional precipitation over Mongolia using a regional climate model. J Hydrol 333:144–154. https://doi.org/10.1016/j.jhydrol.2006.07.023
50. Sazonova TS, Romanovsky VE, Walsh JE, Sergueev DO (2004) Permafrost dynamics in the 20th and 21st centuries along the East Siberian transect. J Geophys Res Atmos 109:. https://doi.org/10.1029/2003JD003680
51. Shinkareva GL, Lychagin MY, Tarasov MK et al (2019) Biogeochemical specialization of macrophytes and their role as a biofilter in the selenga delta. Geogr Environ Sustain 12:240–263. https://doi.org/10.24057/2071-9388-2019-103
52. Sinyukovich VN, Chernyshov MS (2019a) Peculiarities of Long-term Variability of Surface Water Inflow to Lake Baikal. Russ Meteorol Hydrol 44:652–658. https://doi.org/10.3103/S1068373919100029
53. Sinyukovich VN, Chernyshov MS (2017) Transformation of estimated characteristics of the annual and maximal runoff in the major tributaries of Lake Baikal. Water Resour 44:372–379. https://doi.org/10.1134/S0097807817030174
54. Sinyukovich VN, Chernyshov MS (2019b) Water regime of lake Baikal under conditions of climate change and anthropogenic influence. Quat Int 524:93–101. https://doi.org/10.1016/J.QUAINT.2019.05.023
55. Sorokovikova LM, Tomberg IV, Sinyukovich VN et al (2018) Phosphorus in the Selenga River Water and Its Input to Lake Baikal in Conditions of Low Hydraulicity. Geogr Nat Resour 39:343–348. https://doi.org/10.1134/S1875372818040078
56. State report “On the state of Lake Baikal and measures for its protection in 2017”. (2018). Irkutsk: ANO “KC Expert”. 340 p. (In Russian)

57. Sun S, Shi W, Zhou S et al (2020) Capacity of satellite-based and reanalysis precipitation products in detecting long-term trends across Mainland China. Remote Sens 12:2902. https://doi.org/10.3390/RS12182902
58. Thomas BF, Famiglietti JS (2019) Identifying Climate-Induced Groundwater Depletion in GRACE Observations. Sci Rep 9:1–9. https://doi.org/10.1038/s41598-019-40155-y
59. Thorslund J, Jarsjo J, Jaramillo F et al (2017) Wetlands as large-scale nature-based solutions: Status and challenges for research, engineering and management. Ecol Eng 108:489–497. https://doi.org/10.1016/j.ecoleng.2017.07.012
60. Törnqvist R, Jarsjö J, Pietroń J et al (2014) Evolution of the hydro-climate system in the Lake Baikal basin. J Hydrol 519:1953–1962. https://doi.org/10.1016/j.jhydrol.2014.09.074
61. Van Loon AF, Laaha G (2015) Hydrological drought severity explained by climate and catchment characteristics. J Hydrol 526:3–14. https://doi.org/10.1016/j.jhydrol.2014.10.059
62. Wilks DS (2016) “The stippling shows statistically significant grid points”: How research results are routinely overstated and overinterpreted, and what to do about it. Bull Am Meteorol Soc 97:2263–2273
63. Yamazaki D, Ikeshima D, Sosa J et al (2019) MERIT Hydro: A High-Resolution Global Hydrography Map Based on Latest Topography Dataset. Water Resour Res 55:5053–5073. https://doi.org/10.1029/2019WR024873
64. Zongxing L, Qi F, Wang QJ et al (2016) Contributions of local terrestrial evaporation and transpiration to precipitation using δ18O and D-excess as a proxy in Shiyang inland river basin in China. Glob Planet Change 146:140–151. https://doi.org/10.1016/j.gloplacha.2016.10.003
65. Zorigt M, Battulga G, Sarantuya G et al (2019) Runoff dynamics of the upper Selenge basin, a major water source for Lake Baikal, under a warming climate. Reg Environ Chang 19:2609–2619. https://doi.org/10.1007/s10113-019-01564-x

Figures

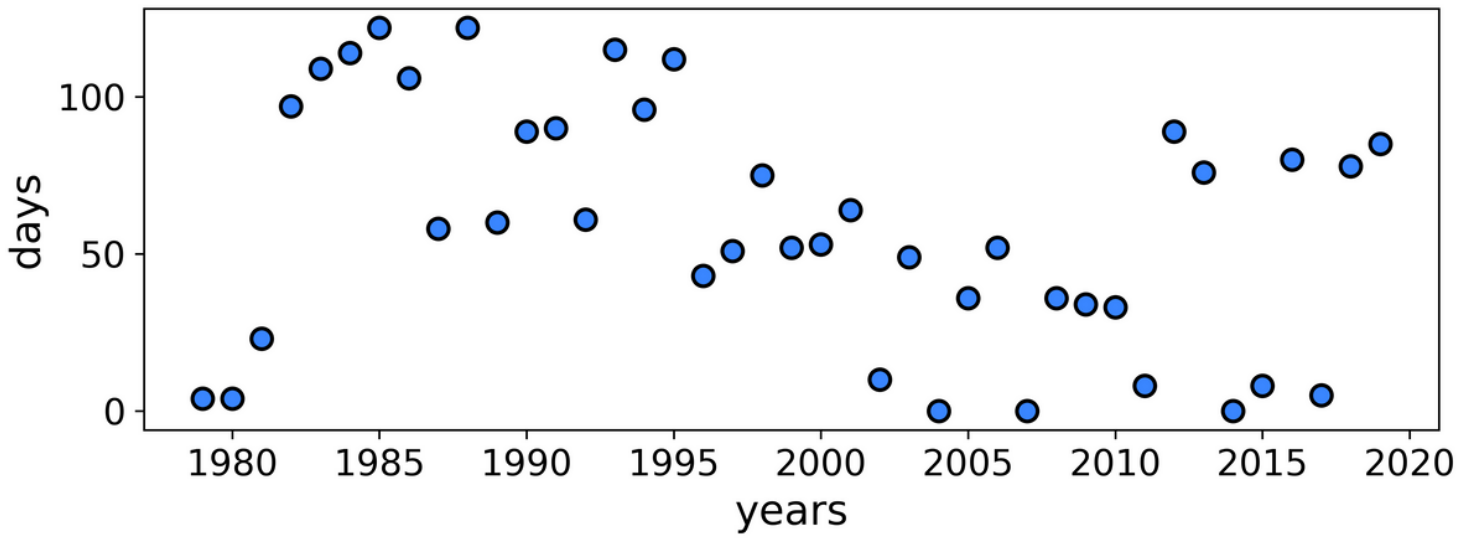

Figure 1

Number of days with discharge above 1350 m3/s at Selenga Mostovoy gauge in June – September.

Figure 2

Location of hydrological gauges and regions in the Baikal catchment used in the present study. See number of gauges in table 1.

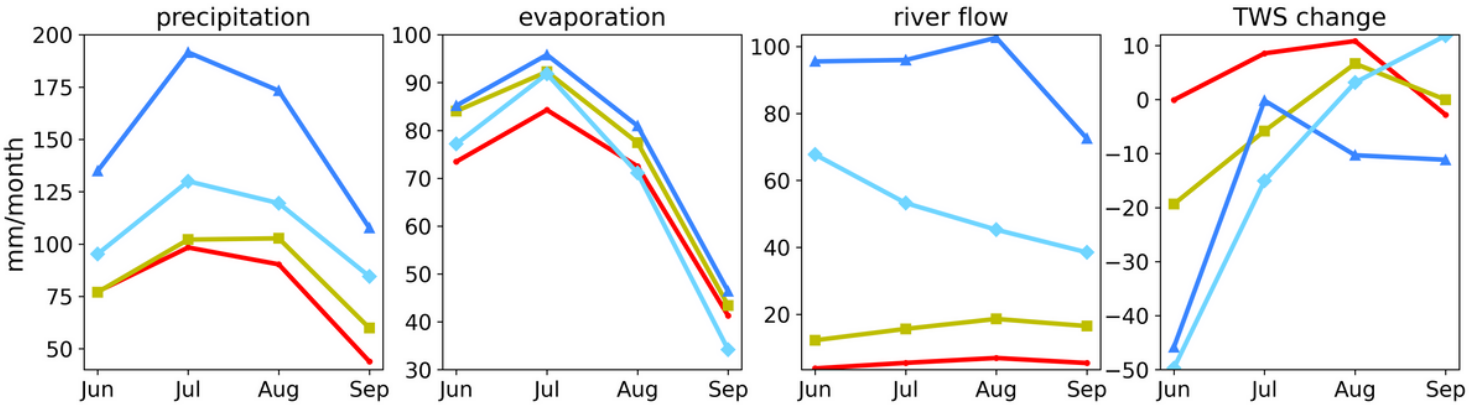

Figure 3

Seasonality of water balance components of the BC. Red line – first region, green line with squares – second region, blue line with triangles – third region blue-green line with rhombuses – fourth region.

Figure 4

Linear rates of change Qflood relative to average Qflood value in BC for 1979–2018, %/year, and their statistical significance

Figure 5

Determination coefficient of linear regression between Qflood and P, E.

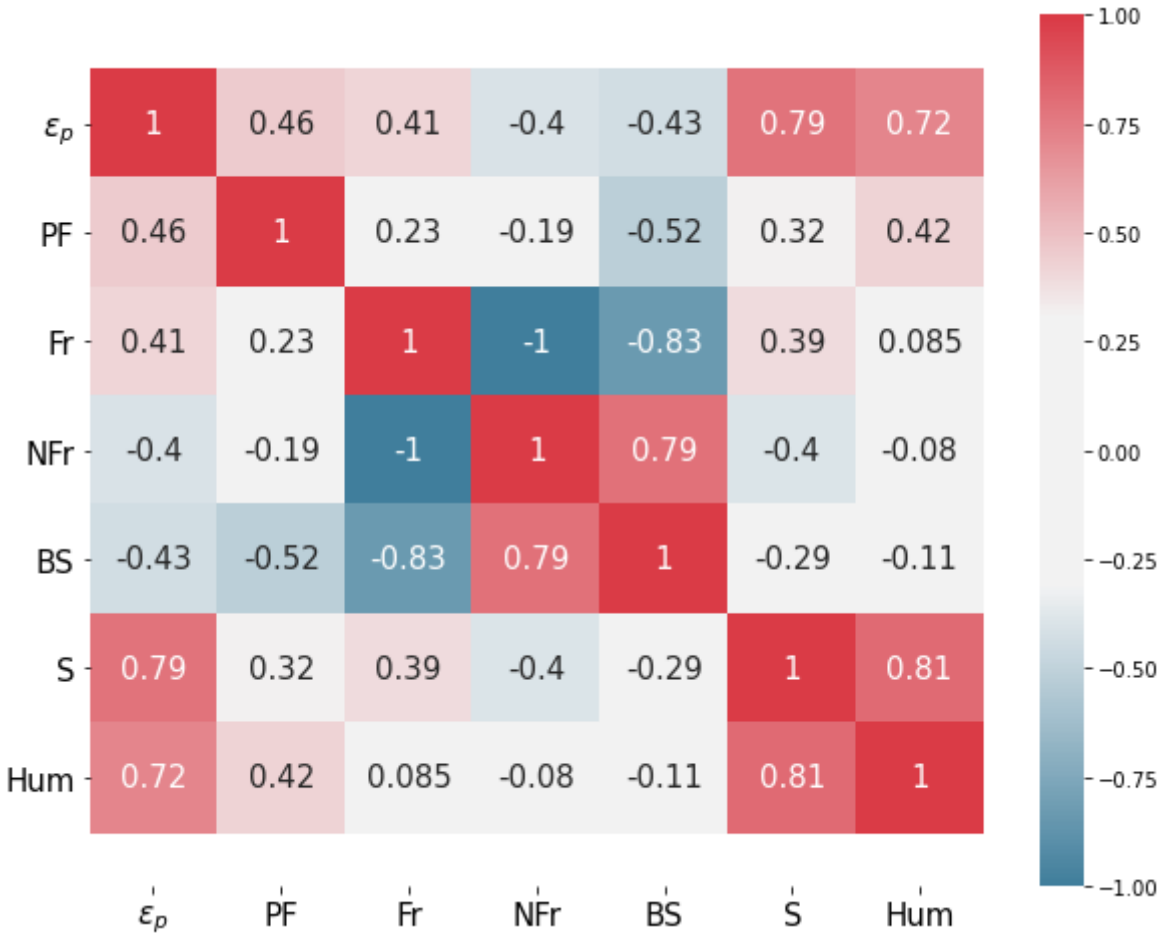

Figure 6

The correlation matrix of untransformed features of catchments and εp.

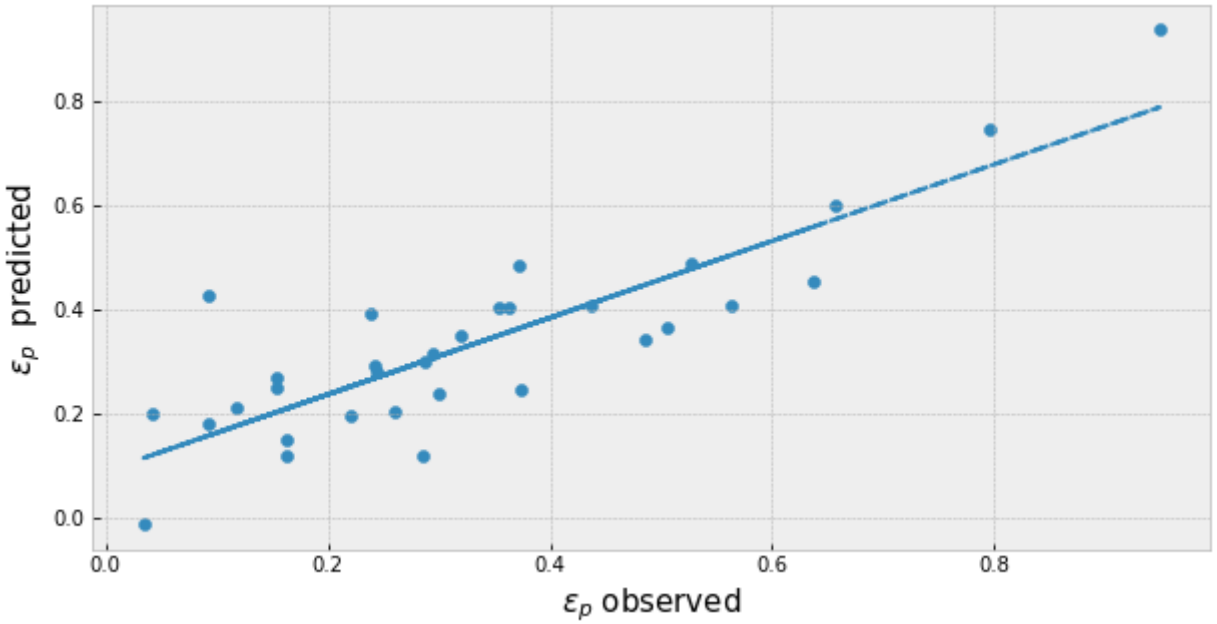

Figure 7

Relationship between εp observed and Eq (3).